Journal of Structural Geology 30 (2008) 767–776

Contents lists available at ScienceDirect

Journal of Structural Geology

journal homepage: www.elsevier.com/locate/jsg

Rheology of dolomite: Large strain torsion experiments and natural examples

Claudio Delle Piane*, Luigi Burlini, Karsten Kunze, Peter Brack, Jean Pierre Burg

Geological Institute ETH, Leonhardstrasse, 19/LEB Zurich, CH-8092, Switzerland

ARTICLE INFO

Article history:
Received 5 September 2007
Received in revised form 9 February 2008
Accepted 24 February 2008
Available online 8 March 2008

Keywords:
Dolomite
Calcite
Deformation
Diffusion creep
Grain boundary sliding
Boudins

ABSTRACT

A set of large strain deformation experiments is presented to better constrain the conditions in which grain size sensitive mechanisms are dominant during deformation of dolomite. Experiments were made on an internally heated gas apparatus equipped with torsion facilities. The rheological data set was fitted to an empirical flow law that allows extrapolation to natural conditions. Fabric evolution with increasing strain was investigated by means of optical and electron microscopy (electron backscattered diffraction). Extrapolation of the laboratory data to geologically relevant conditions of temperature and strain rate was tested on a natural case of a deformed dolomite–calcite sequence across the contact aureole of the Adamello pluton (southern Alps, Italy). Both the geological data and the laboratory measurements indicate that at high temperature an inversion of the relative strength occurs between the two carbonates, with calcite being the weak phase at low temperature and dolomite being the weak phase at high temperature.

1. Introduction

Dolomite, $CaMg(CO_3)_2$, is a very common mineral in the Earth's crust comprising about 10% of all sedimentary rocks. Together with calcite, it plays an important role in the dynamics of the upper crust. Yet in comparison to calcite, deformation experiments on dolomite have received little attention, the conditions that favour different deformation mechanisms in dolomite have not been determined and flow laws describing high temperature creep have been only partially reported (Heard, 1976; Davis et al., in press). In addition, previous high temperature experiments on dolomites were restricted to single crystals (e.g. Barber and Wenk, 1979, 2001; Barber et al., 1981) or to coarse-grained rocks, such as Dover plains dolomite or Crevola dolomite, in which the dominant deformation mechanism included twinning and slip with little evidence of grain size sensitive intergranular deformation mechanisms such as grain boundary diffusion or sliding (Neumann, 1969; Heard, 1976; Barber et al., 1994). Only recently, Davis et al. (in press) quantitatively described the mechanics of plasticity and diffusion creep of dolomite based on deformation experiments on natural coarse-grained dolomite marbles and on synthetic fine-grained aggregates. All of the previous experimental work was limited to small amounts of strain due to the coaxial configuration of their deformation apparatus.

Previous experimental studies, coupled with microstructural analysis, led to the identification of several intracrystalline mechanisms of deformation (Table 1). Dislocation glide occurs mainly on the *c* plane parallel to the *a* direction but also on the *f* and *r* planes, while mechanical twinning is active on the *f* planes (Higgs and Handin, 1959; Barber and Wenk, 1979; Barber et al., 1981; Wenk et al., 1983).

On the other hand, naturally deformed dolomite shows a variety of deformation features so that interpretation of deformation mechanisms based on microstructural considerations has been difficult and often equivocal (e.g. Newman and Mitra, 1994). For example, White and White (1980) reported a TEM study of relatively fine grained (30 μm) dolomite from the Flinton group, south-east Ontario, which underwent deformation under middle amphibolite facies (400–500 MPa and 600 °C). Based on rheological extrapolation and microstructural observations they concluded that grain boundary sliding accompanied by dislocation creep as the primary intracrystalline deformation mechanism, accommodated large amounts of deformation of the fine-grained dolomite.

Field observations often indicate that dolomite is stronger than calcite-rich rocks. Several authors reported the occurrence of fractured dolomite adjacent to limestone and marble showing evidence of plastic deformation (e.g. Woodward et al., 1988; Erickson, 1994). Early experimental studies performed on coarse-grained dolomite, supported the field observations and reported higher fracture and flow strengths for dolomite than for calcite (e.g. Handin et al., 1967). Heard (1976) extrapolated his experimental results to natural strain rates and reported that at deep crustal conditions the flow strengths are largest for dry dunite and dolomite, followed by dry quartzite, marble and wet quarzite.

* Corresponding author. Present address: CSIRO Petroleum Resources, Australian Resources Research Centre, PO Box 1130, Bentley, WA, Australia. Tel.: +61 8 6436 8716; fax: +41 1 632 1080.

E-mail addresses: claudio.dellepiane@csiro.au (C. Delle Piane), burlini@erdw.ethz.ch (L. Burlini), karsten.kunze@emez.ethz.ch (K. Kunze), peter.brack@erdw.ethz.ch (P. Brack), jean-pierre.burg@erdw.ethz.ch (J.P. Burg).

0191-8141/$ – see front matter © 2008 Elsevier Ltd. All rights reserved.
doi:10.1016/j.jsg.2008.02.018

Table 1
Slip and twinning systems of dolomite (modified after Leiss and Barber, 1999)

Slip and twinning systems of dolomite	
c-slip	$(0001)\langle 2\bar{1}\bar{1}0\rangle$
f-slip	$\{\bar{1}012\}\langle 2\bar{2}01\rangle$
r-slip	$\{10\bar{1}4\}\langle \bar{1}2\bar{1}0\rangle$
f-twinning	$\{01\bar{1}2\}\langle 0\bar{1}11\rangle$

1.1. *The Adamello example*

The Adamello pluton is the largest Tertiary intrusion in the Alps and is located north of Brescia (northern Italy). It was emplaced at shallow levels into the southern Alpine crystalline basement and its Permo–Mesozoic sedimentary cover. Inside a narrow border zone and generally at distances <1500 m from the igneous contacts, the country rocks have been subject to thermal alteration during magma emplacement. Peak contact-metamorphism estimates yield temperatures of 600–650 °C along contacts with intermediate to acidic magmatic rocks and between 850 and 900 °C along contacts with mafic rocks (Callegari and Brack, 2002; Matile and Widmer, 1993; Schmid, 1997).

Marbles of different composition and degrees of purity (see Schmid and Flammer, 2002; Berger and Herwegh, 2004) are found in contact with plutonic rocks along the southern border of the Adamello intrusion, and more precisely, in the surroundings of its oldest part, the Re di Castello pluton.

Dolomite marbles and cross-cutting hydrothermal veins show high-temperature, syn-intrusive deformation features (e.g. Brack, 1983) in the innermost part of the contact aureole (see Fig. 1 for exact location). Folds and boudins found in several outcrops at small distance (70 ± 10 m) from the contact with the pluton indicate that calcite behaved as the strong phase relative to dolomite at the time of deformation (Fig. 2). Ptygmatic folds are characterised by a large ratio of amplitude to wavelength, and are formed by highly plastic ductile deformation. They generally represent conditions where the folded material is of a higher viscosity than the surrounding medium (e.g. Ramsay and Huber, 1983). Boudins show different geometries with pinch and swell structures (Fig. 2c) and necked profiles (Fig. 2d) with calcite showing a more viscous behaviour than the dolomitic matrix. Considering a temperature of the intruding rocks of 850 °C, and a distance from the contact of approx. 70 m, the thermal model of Matile and Widmer (1993) indicates that the marbles underwent temperatures of approx. 700 °C. A chemical and microstructural characterization of dolomite marbles from this area is given in Delle Piane et al. (2007).

The field observations described above cannot be explained with the known rheological data from experiments on calcite and dolomite and contradict the assumption that dolomite is always stronger than calcite (e.g. Heard, 1976). Motivated by these occurrences, we undertook an experimental study to better constrain the rheology of dolomite and define its relative strength compared to calcite over a wide set of temperature and strain rate.

2. Sample preparation and experimental methods

2.1. *Starting material*

We used synthetic aggregates made from pure dolomite powder, which was obtained by milling a commercial natural dolomite (Microdol Super provided by Alberto Luisoni Mineralstoffe, Switzerland) for several hours (Herwegh et al., 2003).

The grain size of the starting powder was determined using laser particle analysis, which revealed a three-dimensional particle distribution ranging between 0.4 and 15 μm and a mean of approximately 4 μm (Fig. 3). X-Ray fluorescence and single-point electron microbeam analyses proved that the dolomite powder is extremely pure, with almost stochiometric composition (Table 2).

2.2. *Room-temperature uniaxial press*

Before cold-pressing, the loose powder was dried for at least 24 h in an oven at 120 °C. The powder was cold-pressed into cylindrical stainless steel canisters with an internal diameter of 5.1 cm, length of 20.3 cm, and volume of approx. 415 cm^3, by stepwise filling and pressing of small portions (approx. 20 g) of material. This procedure was designed to eliminate the effect of pressure shadow development and guarantees the homogeneous packing of the powder along the canister length. To avoid excessive

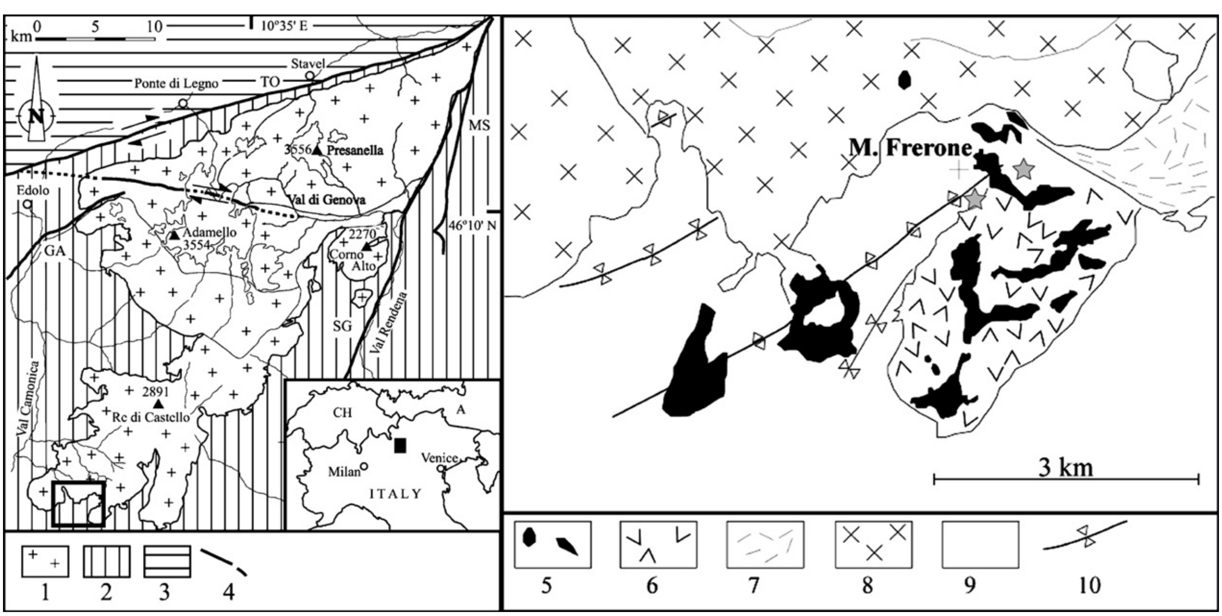

Fig. 1. Geological sketch of the Adamello pluton (redrawn after Di Toro and Pennacchioni, 2004 and Brack, 1983). (1) Composite Adamello batholith; (2) basement and cover of the southern Alps; (3) Austroalpine nappes; (4) major tectonic lines. Right sketch represents an enlargement of the black box in the left map: (5) gabbros and diorite; (6) leucoquarzite; (7) Blumone complex; (8) tonalites; (9) Triassic sediments; (10) major folds. The two stars indicate the location of the structures described in Fig. 2; UTM coordinates 45°56′58.60″N, 10°24′39.70″E.